Supplementary figures and tables

Table S1. Summary of timings of each infection in the 3-step linear regression of annual bromine and MSA at Summit and Tunu. Regression was performed on the data sets with outliers removed as described in Fig. 2. The signs indicate the direction of the inflection in the record, errors are 2σ.

Timing of inflection (Year, C.E.)

	Infl. 1		Infl. 2		Infl. 3		Infl. 4
	Br	MSA	Br	MSA	Br	MSA	Br
Summit-2010	(-)1819 ±22	(-)1854 ±12	(+)1879 ±22	(+)1878 ±12	(+)1932 ±10	(-)1930 ±16	(-)1974 ±20
Tunu	(-)1842 ±22	(-)1812 ±12	(+)1857 ±24	(+)1821 ±21	(+)1944 ±18	(-)1984 ±4	(+)1966 ±20

Table S2. Summary of the average aerosol concentrations as determined by the 3-step linear regression of annual bromine and MSA at Summit and Tunu displayed in Fig. 2. The duration of each step in concentration is bracketed by the inflection points summarized in Table S1. Concentrations are in units of nM. MSA did not show a stable period after the third infection in the series and so was not assigned a concentration value for 'Step 3'. Errors represent 2σ in the concentration value.

Concentration (nM)

	Step 1		Step 2		Step 3
	Br	MSA	Br	MSA	Br
Summit-2010	5.4±0.2	48±1	4.2±0.2	36±2	5.5±0.3
Tunu	4.2±0.3	25±1	3.2±0.3	21.2±0.7	4.8±0.5

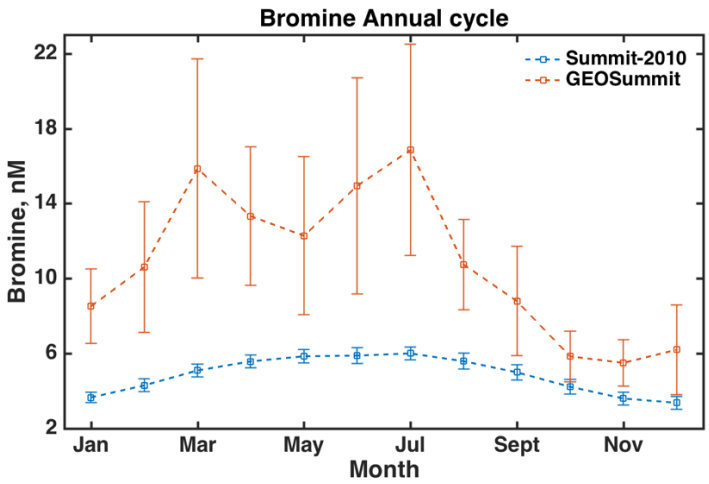

Figure S1. Comparison between the annual cycle in inorganic Br measured at Summit from snow samples taken as part of the GEOSummit project (2007-2013) and in the Summit-2010 ice core (1900-2010). The snow samples were analysed for inorganic Br on the same system used to measure the ice core records. The results of the snow samples support the observation from the ice cores that the maximum flux of Br is in summer with a possible secondary peak in spring. The error bars represent 1σ.

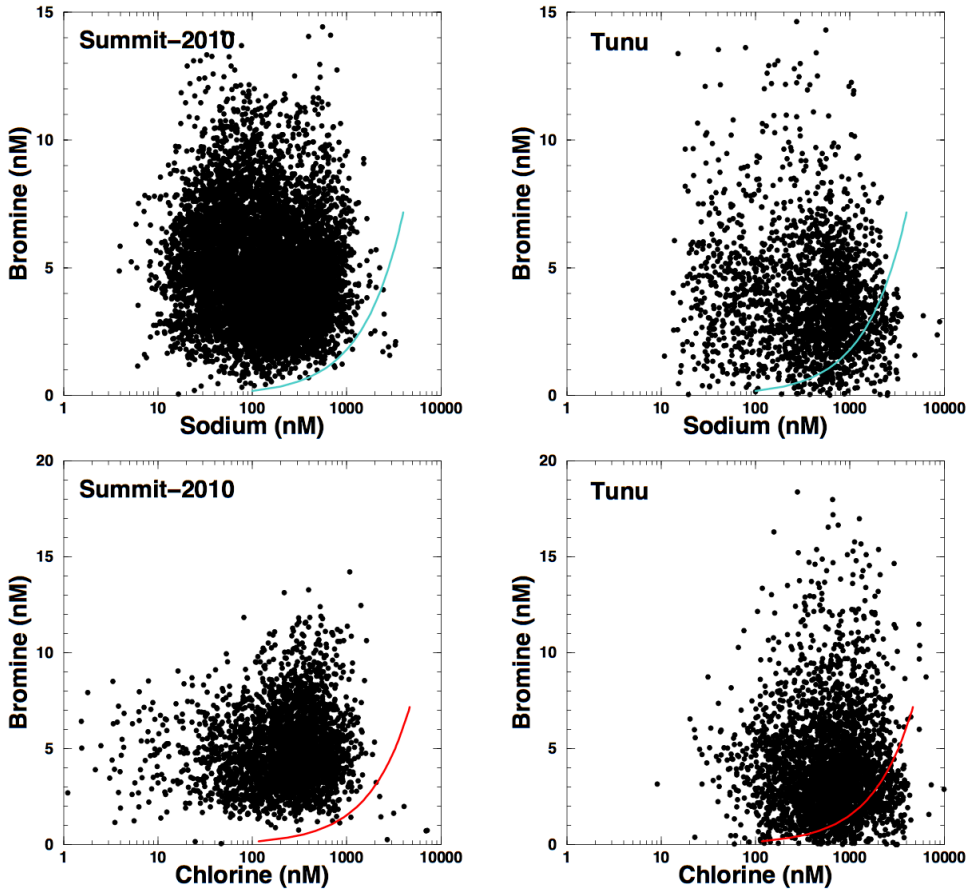

Figure S2. Monthly values of bromine, sodium and chlorine compared with their sea water ratio (coloured lines). At both sites, both the (a) Br/Na and (b) Br/Cl lie predominantly above the sea water ratio. $([Br]/[Na])_{seawater} = 1.793 \times 10^{-3}$, $([Br]/[Cl])_{seawater} = 1.539 \times 10^{-3}$.

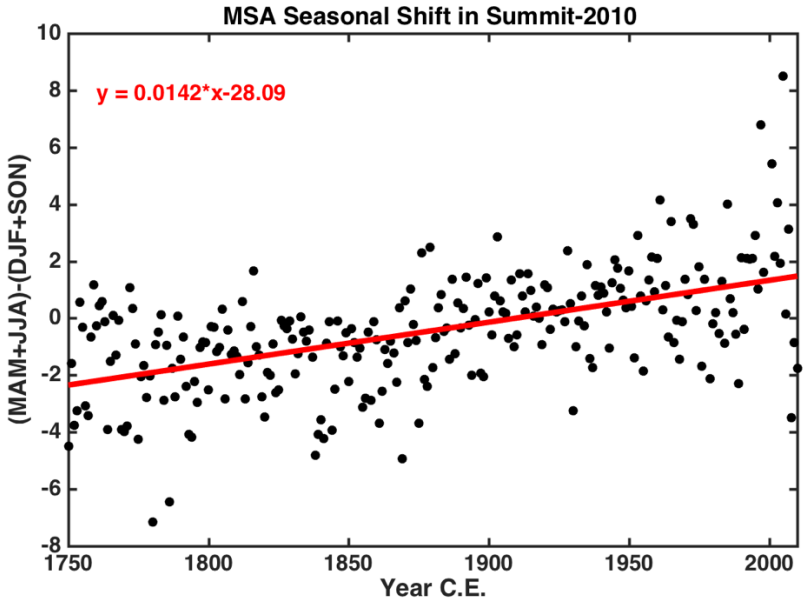

Figure S3. Illustration of the shift in the seasonal MSA peak along the length of the Summit-2010 ice core. The difference in amplitude between the spring/summer and winter/fall MSA signal each year was calculated ((MAM+JJA)-(DJF+SON)) and observed to shift linearly along the length of the icecore. At the shallowest, part of the ice core the positive values show the MSA peak appears in the spring/summer whilst in the deepest and oldest part of the ice core the signal has shifted to a winter/fall annual maximum. This phenomenon has previously been attributed to annual salt gradients within the ice core driving the migration of the MSA toward the higher salt location, winter (Mulvaney et al., 1992; Weller, 2004).

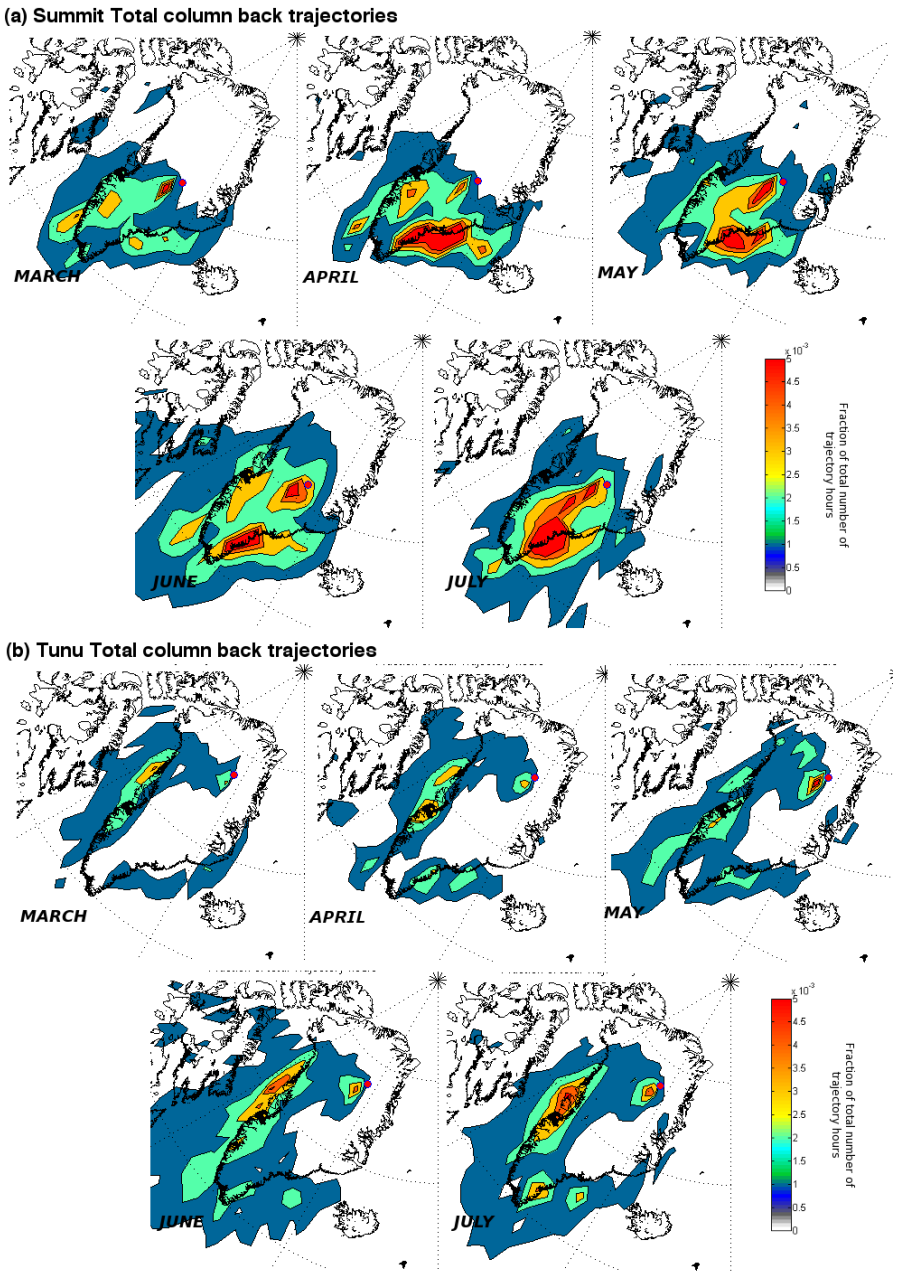

Figure S4. Total column air mass back trajectories from the (a) Summit-2010 and (b) Tunu ice core sites over the period 2005-2013 C.E. Maps display the fraction of the total number of trajectory hours (~100000 hrs month^{-1}) spent within the total vertical column (under 10000 m). Back trajectories were allowed to travel for 10 hours. New trajectories were started every 12 hours. Map grid resolution is 2°x2°. Ice core locations are shown by a pink circle. Maps show that air masses consistently arrive at Summit from the SE Greenland coast with a smaller contribution from the SW coast, consistent with the trajectories seen in the boundary layer (Fig. 6). Air masses consistently arrive at Tunu from the western Greenland coast with a smaller contribution from the SE.

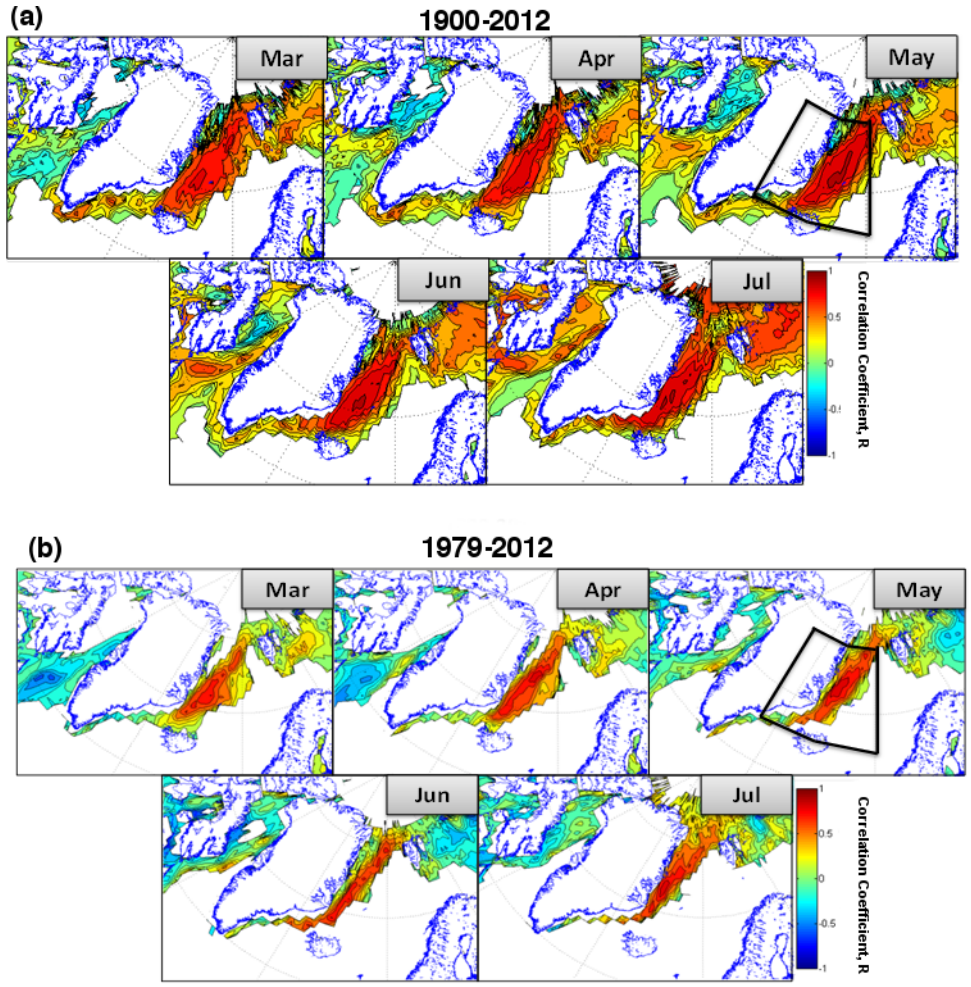

Figure S5. Autocorrelation maps of SIC during (a) the extended era (1900−2012 C.E.) and (b) satellite era (1979−2012 C.E.). Monthly SIC values were compared with the average SIC record from the area which shows the high positive correlation to the Summit-2010 MSA record (outlined in black in Figs. 6a, 6b). There is clearly a negative correlation between sea ice on the east and west coast which is seen over both era from March through to May, but the relationship turns positive in June and July over the extended time period (1900−2012 C.E.)